Received: 4 September 2019 | Revised: 17 January 2020 | Accepted: 22 January 2020

DOI: 10.1111/cas.14337

ORIGINAL ARTICLE

Cancer Science WILEY

Tumor cell-derived angiopoietin-like protein 2 establishes a preference for glycolytic metabolism in lung cancer cells

Hironobu Osumi[1,2] | Haruki Horiguchi[1,3] | Tsuyoshi Kadomatsu[1,4] | Kyosei Tashiro[1] | Jun Morinaga[1] | Takashi Takahashi[5] | Koei Ikeda[2] | Takaaki Ito[6] | Makoto Suzuki[2] | Motoyoshi Endo[7] | Yuichi Oike[1,4]

[1]Department of Molecular Genetics, Graduate School of Medical Science, Kumamoto University, Kumamoto, Japan

[2]Department of Thoracic Surgery, Graduate School of Medical Science, Kumamoto University, Kumamoto, Japan

[3]Institute of Resource Development and Analysis, Kumamoto University, Kumamoto, Japan

[4]Center for Metabolic Regulation of Healthy Aging (CMHA), Graduate School of Medical Sciences, Kumamoto University, Kumamoto, Japan

[5]Aichi Cancer Center, Nagoya, Japan

[6]Department of Pathology and Experimental Medicine, Graduate School of Medical Science, Kumamoto University, Kumamoto, Japan

[7]Department of Molecular Biology, University of Occupational and Environmental Health, Kitakyushu, Japan

Correspondence
Yuichi Oike, Department of Molecular Genetics, Graduate School of Medical Sciences, Kumamoto University, Kumamoto, Japan.
Email: oike@gpo.kumamoto-u.ac.jp

Funding information
Takeda Science Foundation; CREST program of the Japan Agency for Medical Research and Development (AMED), Grant/Award Number: JP19gm0610007; Core Research for Evolutional Science and Technology, Grant/Award Number: 13417915; Ministry of Education, Culture, Sports, Science and Technology, Grant/Award Number: 17K08663, 18K07236 and 18K15246

Abstract

We previously revealed that tumor cell-derived angiopoietin-like protein 2 (ANGPTL2) accelerates the metastatic capacity of tumors in an autocrine/paracrine manner by activating tumor cell motility and invasiveness and the epithelial-mesenchymal transition. However, the effects of ANGPTL2 on cancer cell glycolytic metabolism, which is a hallmark of tumor cells, are unknown. Here we report evidence supporting a role for tumor cell-derived ANGPTL2 in establishing a preference for glycolytic metabolism. We report that a highly metastatic lung cancer cell subline expressing abundant ANGPTL2 showed upregulated expression of the glucose transporter *GLUT3* as well as enhanced glycolytic metabolism relative to a less metastatic parental line. Most notably, ANGPTL2 overexpression in the less metastatic line activated glycolytic metabolism by increasing *GLUT3* expression. Moreover, ANGPTL2 signaling through integrin α5β1 increased *GLUT3* expression by increasing transforming growth factor-β (TGF-β) signaling and expression of the downstream transcription factor zinc finger E-box binding homeobox 1 (ZEB1). Conversely, ANGPTL2 knockdown in the highly metastatic subline decreased *TGF-β1*, *ZEB1*, and *GLUT3* expression and antagonized glycolytic metabolism. In primary tumor cells from patients with lung cancer, *ANGPTL2* expression levels correlated with *GLUT3* expression. Overall, this work suggests that tumor cell-derived ANGPTL2 accelerates activities associated with glycolytic metabolism in lung cancer cells by activating TGF-β-ZEB1-GLUT3 signaling.

KEYWORDS

ANGPTL2, cancer metabolism, GLUT3, lung cancer, ZEB1

1 | INTRODUCTION

The reprogramming of energy metabolism represented by the Warburg effect is a hallmark of cancer.[1] The common feature of such altered cellular metabolism is increased glucose consumption and a shift from oxidative phosphorylation to glycolysis.[2] Increased rates of glycolysis provide cancer cells with growth and survival advantages and are associated with tumor aggressiveness and malignancy.[3,4] The GLUT (*SLC2A*) family of glucose transporter proteins is a key regulator of glucose uptake across cell membranes.[5] Among its 14 members, GLUT1 is broadly expressed in various cancer cells and plays a pivotal role in glycolytic metabolism.[6] Interestingly, a recent report indicates that GLUT3 is also expressed in glioblastoma,[7] colon cancer,[8] and lung cancer,[9] suggesting that GLUT3 also functions in metabolic activity in cancer cells.

The epithelial-mesenchymal transition (EMT) plays essential roles in development, tissue regeneration, wound healing, and organ fibrosis.[10] Transforming growth factor-β (TGF-β) functions to induce EMT[11,12] by increasing expression of the transcription factors Snail and zinc finger E-box binding homeobox 1 (ZEB1), which repress epithelial markers such as E-cadherin, and by inducing mesenchymal markers, such as vimentin.[13,14] In tumor cells, the EMT is associated with increased tumor cell invasion and metastasis.[15] Interestingly, recent studies indicate that the EMT promotes changes in cancer metabolism, antagonizes cancer cell apoptosis and senescence, and increases immunosuppression.[10,16]

We have reported that angiopoietin-like protein 2 (ANGPTL2), which functions as a proinflammatory mediator in various diseases, including cancer,[17] promotes the EMT by activating the TGF-β pathway in a chemically induced skin squamous cell carcinoma mouse model.[18] We also showed that, in an autocrine/paracrine manner, tumor cell-derived ANGPTL2 accelerates aggressive metastatic phenotypes in tumor cells by activating cell motility, invasiveness, and the EMT in human lung and breast cancers and osteosarcoma.[19-21] However, ANGPTL2 function has not been studied in the context of cancer cell metabolism.

Here, we report that, in primary tumor cells from patients with lung cancer, *ANGPTL2* expression levels positively correlate with those of *GLUT3*, but not *GLUT1*. Our in vitro analysis using lung cancer cell lines revealed that tumor cell-derived ANGPTL2 signaling through integrin α5β1 increases *GLUT3* expression by activating the TGF-β-ZEB1 pathway, thereby activating glycolytic metabolism in lung cancer cells.

2 | MATERIALS AND METHODS

2.1 | Human studies

Tissue samples were resected from 96 lung cancer patients at the Department of Thoracic Surgery of Kumamoto University Hospital. All specimens were diagnosed as lung cancer by a pathologist. All studies were approved by the Ethics Committee of Kumamoto University.

2.2 | Immunohistological staining

Formalin-fixed, paraffin-embedded specimens were cut into 4-μm sections and deparaffinized. Sections were autoclaved with citrate buffer (pH 6.0) for antigen retrieval. Sections were incubated with 3% H_2O_2 for 5 minutes to block endogenous peroxidase activity and then incubated with anti-ANGPTL2 Ab and anti-GLUT3 (1:100, HPA006539; Sigma-Aldrich), diluted with Block Ace (KAC) at 4°C overnight. After washing with PBS, sections were incubated for 30 minutes with EnVision+ System-HRP-labeled Polymer Anti-rabbit (Dako) for visualization with DAB (Dojindo). Slides were counterstained 20 seconds with hematoxylin.

2.3 | Total RNA extraction and real-time quantitative RT-PCR

Total RNA was isolated from cells using TRIzol reagent (Invitrogen) and from human tissue samples using the Total RNA Extraction Miniprep System (Viogene). DNase-treated RNA was reversed-transcribed using a PrimeScript RT reagent kit (Takara Bio). The PCR products were analyzed using a Thermal Cycler Dice Real Time System (Takara Bio). The PCR primer sequences are shown in Table S1. Relative transcript abundance was normalized to that of *RPS18* mRNA.

2.4 | Cell culture

The human lung cancer lines NCI-H460 (H460) and NCI-H460-LNM35 (LNM35) were previously described[22] and provided by Dr T. Takahashi (Aichi Cancer Center, Japan). NCI-H1975 (H1975) was purchased from ATCC. HCC15 (H15) was established at the Hamon Center for Therapeutic Oncology Research, University of Texas Southwestern Medical Center[23] and generously donated by Dr Adi F. Gazdar (University of Texas Southwestern Medical Center). H460, LNM35, H1975, and H15 cells were cultured in RPMI-1640 medium supplemented with 10% FCS at 37°C in a humidified 5% CO_2 atmosphere. For some experiments, cells were treated with 10 μM MEK inhibitor U0126 (662005; Millipore) for 6 h in normal growth medium.

2.5 | Plasmid transfection

For stable transfection, H460, H1975, and H15 cells were transfected with ANGPTL2 or empty vectors[24] using Lipofectamine 2000 (Invitrogen) according to the manufacturer's protocol and selected in 400-800 μg/mL G418.

2.6 | Immunoblot analysis

Solubilized proteins were subjected to SDS-PAGE, and proteins were electrotransferred to PVDF membranes. Immunoblotting was carried out with Abs against ANGPTL2 (1:2000, BAF1444; R&D

Systems) and Hsc70 (1:2000, #sc7298; Santa Cruz Biotechnology). Immunodetection was carried out using an ECL kit (GE Healthcare) according to the manufacturer's protocol.

2.7 | Flow cytometry

Cells were suspended in MACS buffer (Miltenyi Biotec) and stained with the following Abs: anti-GLUT3 (ab15311; Abcam), anti-integrin α5β1 (MAB1969; Millipore), anti-integrin αvβ3 (MAB1976Z; Millipore), anti-integrin αvβ5 (MAB1961; Millipore), and anti-integrin α9β1 (Sc-59969; Santa Cruz Biotechnology). Cells were incubated with appropriate secondary Abs. Viable cells were identified as unstained with 7-AAD (Beckman Coulter). Stained cells were analyzed by BD FACSVerse (BD Biosciences). Data analysis was undertaken using FlowJo software (TreeStar).

2.8 | Glucose uptake and lactate production assays

Glucose uptake was determined using a Glucose Uptake-Glo Assay (Promega) and lactate production by using a Lactate Assay Kit-WST (Dojindo), according to each manufacturer's protocols.

2.9 | Immunofluorescence

For ZEB1 staining, cells were first fixed for 20 minutes in acetone and ethanol (1:1) and then blocked in 5% normal goat serum (Nichirei Biosciences). Cells were incubated with anti-ZEB1 Abs (1:50, #sc515797; Santa Cruz Biotechnology) and then with Alexa 488-conjugated anti-mouse Abs. Nuclei were counterstained with DAPI.

2.10 | Knockdown of ZEB1

H460 cells were reseeded in 12-well plates and transfected with *ZEB1* siRNA (SYK [ID SR304746] Trilencer-27 human siRNA; OriGene). As a control, we used Trilencer-27 Universal Scrambled Negative Control (OriGene). Total RNA was extracted for quantitative RT-PCR (qRT-PCR) analysis 24 hours later.

2.11 | Knockdown of ANGPTL2

ANGPTL2-specific knockdown LNM35 cells was described previously.[19]

2.12 | Statistical analyses

Statistical analyses were undertaken using GraphPad Prism 8 software (GraphPad Software). Statistical parameters and methods are reported in figures and corresponding legends. Results with *P* values less than .05 were considered significant (**P* < .05; ***P* < .01; ****P* < .001). Comparisons between 2 groups were carried out using the unpaired 2-tailed *t* test. Comparisons between 3 or more groups were undertaken using one-way ANOVA with Tukey's multiple comparison test. Potential correlations of *ANGPTL2*, GLUT1 (*SLC2A1*), GLUT3 (*SLC2A3*), or *ZEB1* expression in lung cancer specimens were evaluated by calculating Spearman's correlation coefficient.

3 | RESULTS

3.1 | Glucose transport 3 abundantly expressed in aggressive lung cancer cells

The NCI-H460-LNM35 (LNM35) line is a highly metastatic subline of the human large-cell lung carcinoma cell line NCI-H460 (H460).[22] Because enhanced glycolytic metabolism is reportedly associated with tumor aggressiveness,[4,25] we asked whether LNM35 and H460 cells differed in terms of glycolytic metabolism by comparing glucose uptake and lactate production in both lines. Both glucose uptake and lactate production were significantly increased in LNM35 relative to H460 cells (Figure 1A,B), suggesting activation of glycolytic metabolism in the highly metastatic line.

As GLUT family glucose transporters are critical for glucose transport and reportedly contribute to tumor progression in various cancers, including lung cancer,[6,26,27] we compared expression levels of *GLUT1* (*SLC2A1*), *GLUT2* (*SLC2A2*), *GLUT3* (*SLC2A3*), and *GLUT4* (*SLC2A4*) in H460 and LNM35 cells. Interestingly, *GLUT1*, *GLUT2*, and *GLUT4* expression was comparable in both lines, whereas expression levels of *GLUT3* in LNM35 cells were significantly higher than in H460 cells (Figure 1C). To further investigate factors potentially accelerating glucose uptake and lactate production in LNM35 cells, we compared expression of transcripts encoding the glycolytic enzymes hexokinase 1 (*HK1*), hexokinase 2 (*HK2*), phosphofructokinase muscle (*PFKM*), phosphofructokinase platelets (*PFKP*), aldolase fructose-bisphosphate a (*ALDOA*), phosphoglycerate kinase 1 (*PGK1*), enolase 1 (*ENO1*), enolase 2 (*ENO2*), pyruvate kinase M (*PKM*), and lactate dehydrogenase A (*LDHA*) in H460 and LNM35 cells (Figure 1D). Quantitative RT-PCR analysis revealed that *PFKP*, *ALDOA*, *PGK1*, *PKM*, and *LDHA* mRNA levels were slightly higher in LNM35 cells than in H460 cells. These results suggest that enhanced glycolytic metabolism seen in LNM35 cells might be primarily attributable to increased GLUT3 expression in LNM35 relative to H460 cells.

3.2 | Angiopoietin-like protein 2 expression induces GLUT3 expression and enhances glycolytic metabolism in lung cancer cells

We previously reported that increased metastatic ability of LNM35 relative to H460 cells is due to significant activation of ANGPTL2-dependent tumor cell motility and invasiveness in LNM35 cells.[19]

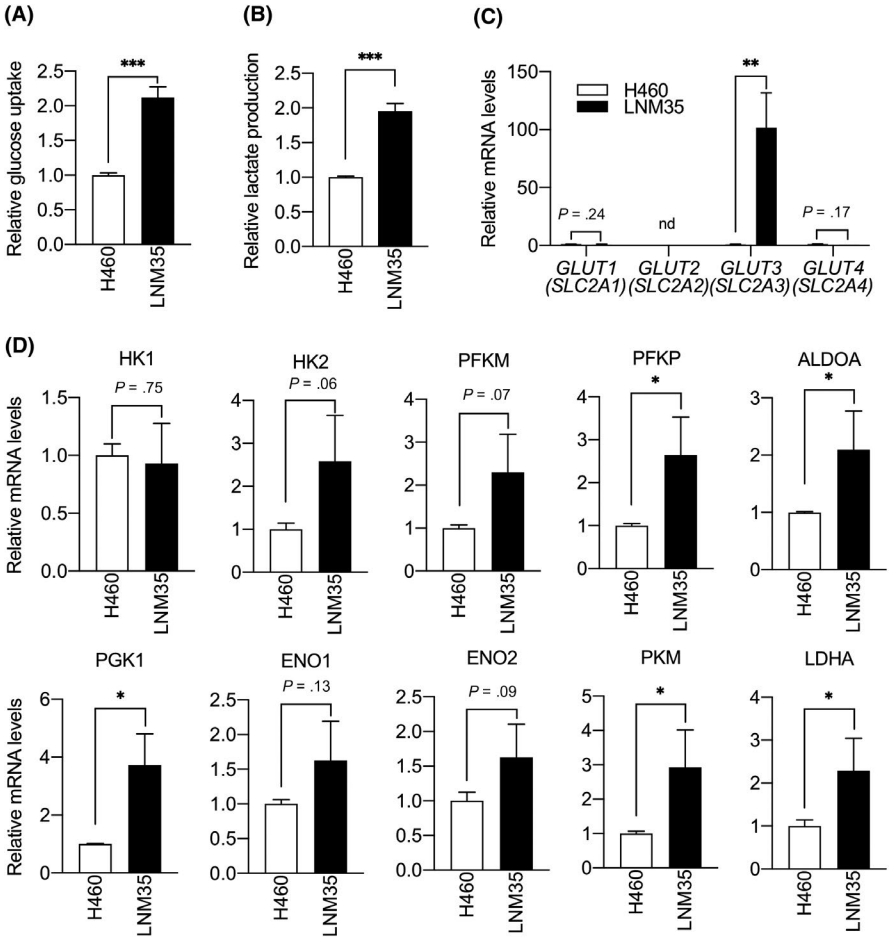

FIGURE 1 Aggressive lung cancer cells show increased glycolytic metabolism and glucose transporter 3 (GLUT3) expression. A, Relative glucose uptake in H460 and LNM35 cells. Levels in H460 cells were set to 1. Data are means ± SD; n = 3 per group. ***P < .001, unpaired t test. B, Relative lactate production in H460 and LNM35 cells. Levels in H460 cells were set to 1. Data are means ± SD; n = 4 per group. ***P < .001, unpaired t test. C, Comparison of levels of GLUT1-4 (*SLC2A1-4*) transcripts in H460 and LNM35 cells. Levels in H460 cells were set to 1. Data are means ± SD; n = 3 per group. nd, not detected. **P < .01, unpaired t test. D, Comparison of levels of indicated transcripts in H460 and LNM35 cells. Levels in H460 cells were set to 1. Data are means ± SD; n = 3 per group. *P < .05, unpaired t test. ALDOA, aldolase fructose-bisphosphate A; ENO, enolase; HK, hexokinase; LDHA, lactate dehydrogenase A;PFKM, phosphofructokinase muscle; PFKP, phosphofructokinase platelets; PGK1, phosphoglycerate kinase 1; PKM, pyruvate kinase M

Accordingly, *ANGPTL2* transcripts were more abundant in LNM35 than in H460 cells (Figure 2A). Here, we also found that LNM35 cells show increased *GLUT3* expression and enhanced glycolytic metabolism compared to H460 cells, as shown in Figure 1. These findings suggest that ANGPTL2 activity is linked to metabolic preference in tumor cells. To assess this possibility, we established 2 independent H460 cell lines, 1 overexpressing ANGPTL2 (H460/ANGPTL2) and the other a control H460 line overexpressing empty vector (H460/vector) (Figure 2B), and compared glucose uptake and lactate production in both (Figure 2C,D). Glucose uptake and lactate production in H460/ANGPTL2 lines were significantly increased relative to corresponding activities in control H460/vector cells. Moreover, expression levels of *GLUT3*, but not *GLUT1*, in the H460/ANGPTL2 line was markedly increased relative to expression in control H460/

FIGURE 2 Angiopoietin-like protein 2 (ANGPTL2) increases glucose transporter 3 (GLUT3) expression and glycolytic metabolism. A, Comparison of levels of *ANGPTL2* transcripts in H460 and LNM35 cells. Levels in H460 cells were set to 1. Data are means ± SD; n = 3 per group. *P < .05, unpaired t test. B, Representative immunoblotting for ANGPTL2 in H460/ANGPTL2 and H460/vector cells. Heat shock cognate protein 70 (HSC70) served as a loading control. C, Relative glucose uptake in H460/ANGPTL2 and H460/vector cells. Levels in H460/vector cells were set to 1. Data are means ± SD; n = 6 per group. *P < .05, **P < .01, one-way ANOVA test followed by Tukey's multiple comparison test. D, Relative lactate production in H460/ANGPTL2 and H460/vector cells. Levels in H460/vector cells were set to 1. Data are means ± SD; n = 3 per group. ***P < .001, one-way ANOVA test followed by Tukey's multiple comparison test. E, Comparison of levels of GLUT1 (*SLC2A1*) and GLUT3 (*SLC2A3*) transcripts in H460/ANGPTL2 and H460/vector cells. Levels in H460/vector cells were set to 1. Data are means ± SD; n = 3 per group. **P < .01, one-way ANOVA test followed by Tukey's multiple comparison test. F, Representative profiles showing cell surface expression of GLUT3 (black line traces) or isotype-matched control (gray filled traces) in H460/ANGPTL2 and H460/vector cells, as assessed by flow cytometry analysis. Gating of living cells was carried out after background assessment. MFI, median fluorescence intensity. G, Representative immunoblotting for ANGPTL2 in H1975/ANGPTL2 and H1975/vector cells, and in H15/ANGPTL2 and H15/vector cells. HSC70 served as a loading control. H, I, Relative glucose uptake and lactate production in H1975/ANGPTL2 and control cells, and H15/ANGPTL2 and control cells. Levels in respective vector control cells were set to 1. Data are means ± SD; n = 3 per group. **P < .01, ***P < .001, one-way ANOVA test followed by Tukey's multiple comparison test. J, K, Comparison of levels of GLUT1 (*SLC2A1*) and GLUT3 (*SLC2A3*) transcripts in H1975/ANGPTL2 and control cells, and H15/ANGPTL2 and control cells. Levels in respective vector control cells were set to 1. Data are means ± SD; n = 3 per group. **P < .01, ***P < .001, one-way ANOVA test followed by Tukey's multiple comparison test

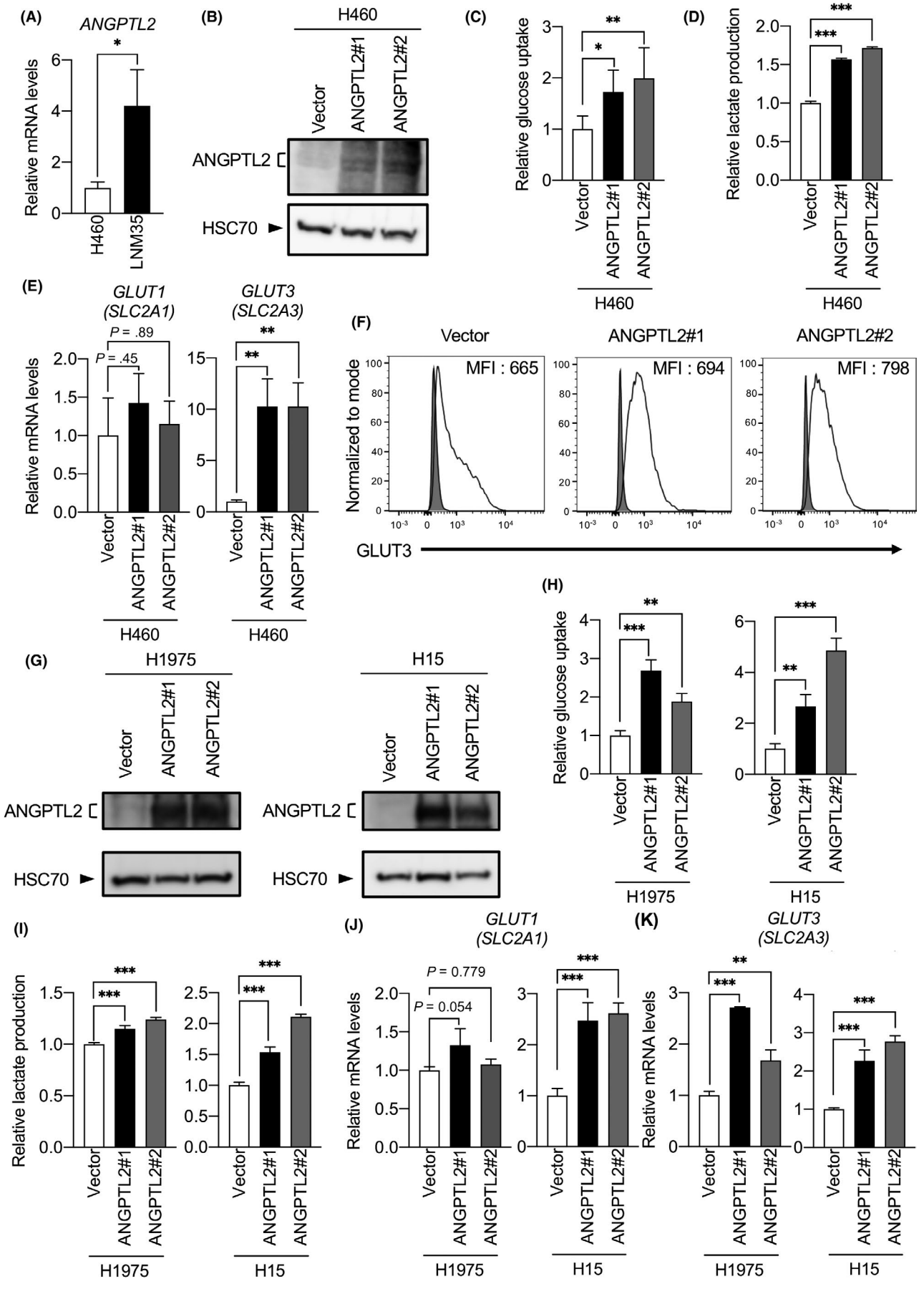
(A)
ANGPTL2
Relative mRNA levels
H460
LNM35
(B)
H460
Vector
ANGPTL2#1
ANGPTL2#2
ANGPTL2
HSC70
(C)
Relative glucose uptake
H460
(D)
Relative lactate production
H460
(E)
GLUT1 (SLC2A1)
GLUT3 (SLC2A3)
P = .89
P = .45
Relative mRNA levels
H460
(F)
Vector
ANGPTL2#1
ANGPTL2#2
MFI : 665
MFI : 694
MFI : 798
Normalized to mode
GLUT3
(G)
H1975
H15
ANGPTL2
HSC70
(H)
Relative glucose uptake
H1975
H15
(I)
Relative lactate production
H1975
H15
(J)
GLUT1 (SLC2A1)
P = 0.779
P = 0.054
Relative mRNA levels
H1975
H15
(K)
GLUT3 (SLC2A3)
Relative mRNA levels
H1975
H15

vector cells (Figure 2E). Consistently, FACS analysis with an anti-GLUT3 Ab revealed an increase in GLUT3 protein levels on the surface of H460/ANGPTL2 relative to control H460/vector cells (Figure 2F).

To assess whether ANGPTL2 activity alters *GLUT3* expression in other lung cancer lines, we established 2 additional ANGPTL2-overexpressing lines plus corresponding controls: the human lung adenocarcinoma line H1975 (H1975/ANGPTL2 and H1975/vector) and the human lung squamous cell carcinoma line H15 (H15/ANGPTL2 and H15/vector) (Figure 2G). As in H460 cells, glucose uptake and lactate production in H1975/ANGPTL2 and H15/ANGPTL2 lines were significantly increased relative to corresponding controls (Figure 2H,I). Quantitative RT-PCR revealed that expression levels of *GLUT3* in H1975/ANGPTL2 and H15/ANGPTL2 were higher than in control cells (Figure 2J,K). Taken together, these results suggest that ANGPTL2 enhances glycolytic metabolism in lung cancer cells by increasing GLUT3-dependent glucose transport.

3.3 | Angiopoietin-like protein 2 induces GLUT3 expression through the TGF-β–ZEB1 pathway

We next asked how ANGPTL2 increases *GLUT3* expression in lung cancer cells. Glucose transporter 3 transcription is reportedly regulated by the DNA binding protein ZEB1, which is upregulated by TGF-β signaling during the EMT in nonsmall-cell lung cancer cells.[26] Furthermore, we previously reported that ANGPTL2 promotes the EMT by activating the TGF-β pathway.[18] Based on these findings, we hypothesized that ANGPTL2 induces *GLUT3* expression in lung cancer cells by activating TGF-β-induced ZEB1 expression. To assess this possibility, we first investigated the EMT status of H460/ANGPTL2 and H460/vector control cells (Figure 3A). Expression levels of *CDH1* (E-cadherin), an epithelial marker, in H460/ANGPTL2 cells were markedly lower than those seen in control H460/vector cells. By contrast, expression levels of *VIM* (vimentin), a mesenchymal marker, in H460/ANGPTL2 cells were significantly higher than those seen in control H460/vector cells. Consistently, we found significantly increased expression of *TGFB1* (TGF-β1) and the EMT-associated transcription factors *ZEB1* and *SNAI1* in H460/ANGPTL2 relative to control H460/vector cells (Figure 3B). Furthermore, *TGFB1* and *ZEB1* transcript levels were higher in H1975/ANGPTL2 and H15/ANGPTL2 than in corresponding control cells (Figure 3C,D). We also observed increased nuclear accumulation of ZEB1 in H460/ANGPTL2 relative to control H460/vector cells (Figure 3E,F). These results suggest that tumor cell-derived ANGPTL2 increases GLUT3 expression by activating both the TGF-β1-ZEB1 pathway and the EMT.

We then asked whether *GLUT3* expression in lung cancer cells changes after suppression of *ZEB1* expression in H460/ANGPTL2 and H460/vector cells. To do so, we transfected both lines with either *ZEB1*-specific siRNAs (siZEB1#1 and siZEB1#2) or control scramble siRNA (siControl) (Figure 3G,H). *ZEB1* knockdown in H460/ANGPTL2 cells significantly decreased *GLUT3* expression, whereas we observed no change in *GLUT3* expression in siControl-transfected H460/ANGPTL2 cells (Figure 3H). Interestingly, we observed no change in *GLUT3* expression in H460/vector cells, even in *ZEB1* knockdown cells (Figure 3G,H). Thus, we conclude that increased *GLUT3* expression due to ANGPTL2 expression is due to ZEB1 upregulation, suggesting that ANGPTL2 activates the TGF-β-ZEB1 pathway and increases GLUT3 expression.

3.4 | Angiopoietin-like protein 2 signaling through integrin α5β1 increases ZEB1-mediated GLUT3 expression

We next assessed molecular mechanisms underlying ANGPTL2-mediated activation of the TGF-β-ZEB1 pathway. As ANGPTL2 signaling through integrin α5β1 enhances cancer cell metastasis, including EMT activation,[20,21] we evaluated integrins expressed on the H460 cell surface by flow cytometry. As shown in Figure 4A, integrin α5β1 is expressed on H460 cells, suggesting that ANGPTL2 activates TGF-β-ZEB1 signaling through this receptor. Accordingly, *TGFB1* and *ZEB1* expression significantly decreased in H460/ANGPTL2 cells treated by an anti-integrin α5β1 blocking Ab (α5β1 Ab) as compared to a control IgG-treated (cIgG) group (Figure 4B). Signaling through the ANGPTL2-integrin α5β1 axis reportedly activates ERK signaling and subsequent TGF-β expression.[28] Indeed, qRT-PCR analysis revealed that *TGFB1* transcript levels were significantly decreased following treatment of H460/ANGPTL2 cells with the MEK inhibitor U0126 (Figure 4C), suggesting that ANGPTL2 could upregulate *TGFB1* through integrin α5β1-ERK signaling. Furthermore, *GLUT3* induction in H460/ANGPTL2 cells was significantly suppressed after cells were treated with integrin α5β1 blocking Ab (Figure 4D). Collectively, these results suggest that tumor cell-derived ANGPTL2 autocrine/paracrine signaling through integrin α5β1 increases GLUT3 expression by activating the TGF-β-ZEB1 pathway.

3.5 | Angiopoietin-like protein 2 knockdown reduces glycolytic metabolism in aggressive lung cancer cells

To confirm ANGPTL2 function in metabolic reprogramming of lung cancer cells, we generated 3 independent LNM35 cell sublines expressing a microRNA-mediated RNA interference expression vector designed to knockdown *ANGPTL2*, namely, miANGPTL2#1, miANGPTL2#2, and *LacZ* (miLacZ) (Figure 5A). Expression of *TGFB1*, *ZEB1*, and *GLUT3* in both LNM35/miANGPTL2#1 and LNM35/miANGPTL2#2 cells was significantly decreased relative to LNM35/miLacZ cells (Figure 5B,C). Moreover, glucose uptake and lactate production in both LNM35/miANGPTL2#1 and LNM35/miANGPTL2#2 cells were significantly reduced compared to levels seen in control LNM35/miLacZ cells (Figure 5D,E). We conclude that tumor cell-derived ANGPTL2 autocrine/paracrine signaling drives glycolytic metabolism phenotypes in lung cancer cells.

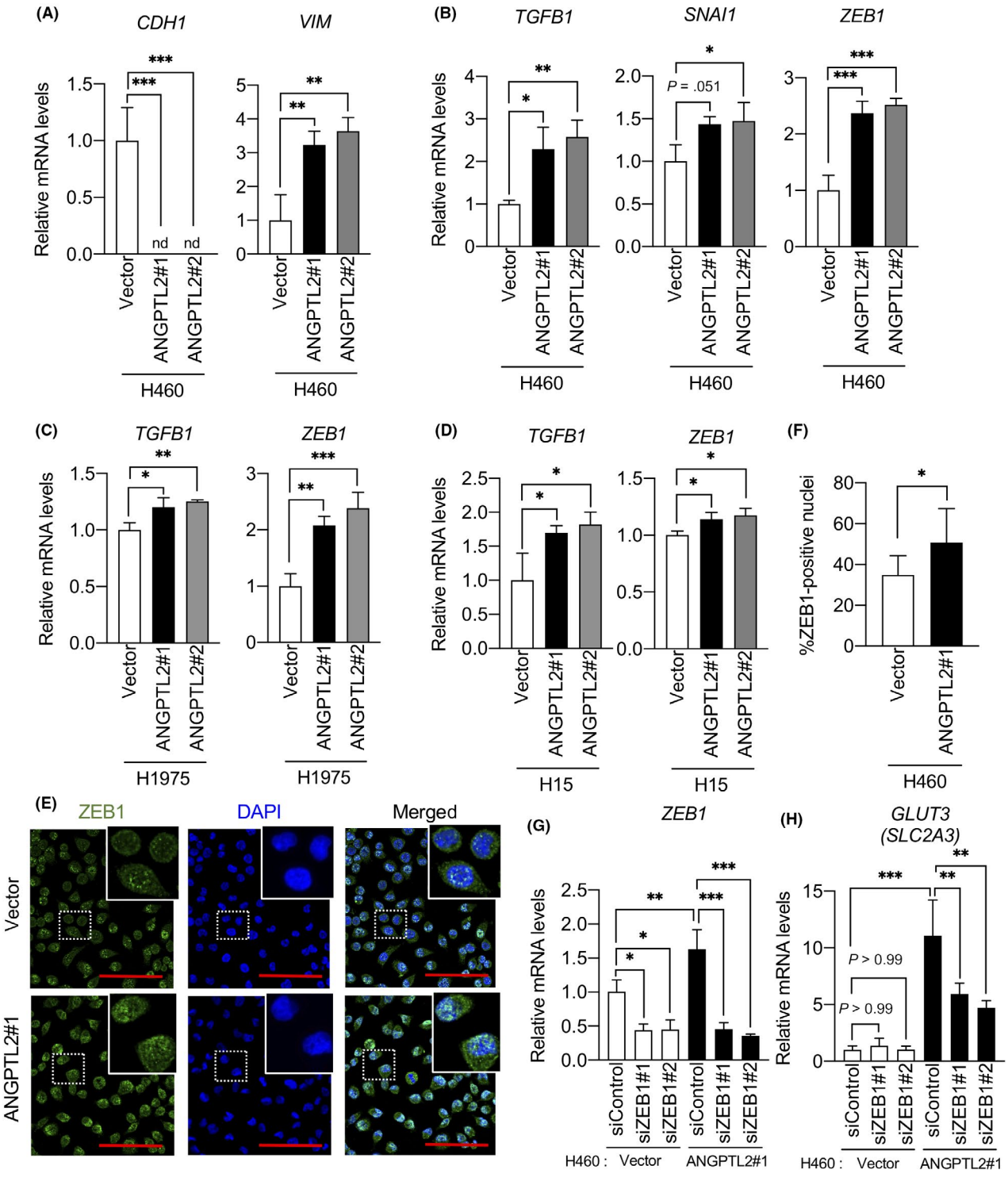

FIGURE 3 Angiopoietin-like protein 2 (ANGPTL2) induces glucose transporter 3 GLUT3 expression through zinc finger E-box binding homeobox 1 (ZEB1). A, B, Comparison of levels of indicated transcripts in H460/ANGPTL2 and H460/vector cells. Levels seen in H460/vector cells were set to 1. Data are means ± SD; n = 3 per group. *$P < .05$, **$P < .01$, ***$P < .001$, one-way ANOVA test followed by Tukey's multiple comparison test. C, D, Comparison of levels of indicated transcripts in H1975/ANGPTL2 and control cells, and in H15/ANGPTL2 and control cells. Levels in respective vector control cells were set to 1. Data are means ± SD; n = 3 per group. *$P < .05$, **$P < .01$, ***$P < .001$, one-way ANOVA test followed by Tukey's multiple comparison test. E, Immunofluorescent staining for ZEB1 (green) in H460/ANGPTL2 and H460/vector cells. Nuclei are counterstained with DAPI (blue). Scale bar = 100 μm. Insets show magnified images. F, Quantification of ZEB1-positive nuclei. Data are means ± SD; n = 8 per group. *$P < .05$, unpaired *t* test. G, H, Comparison of levels of indicated transcripts in H460/ANGPTL2 and H460/vector cells transfected with ZEB1-specific siRNAs (siZEB1#1 or siZEB1#2) or negative control siRNA (siControl). Levels in control siRNA H460/vector cells were set to 1. Data are means ± SD; n = 3 per group. *$P < .05$, **$P < .01$, ***$P < .001$, one-way ANOVA followed by Tukey's multiple comparison test

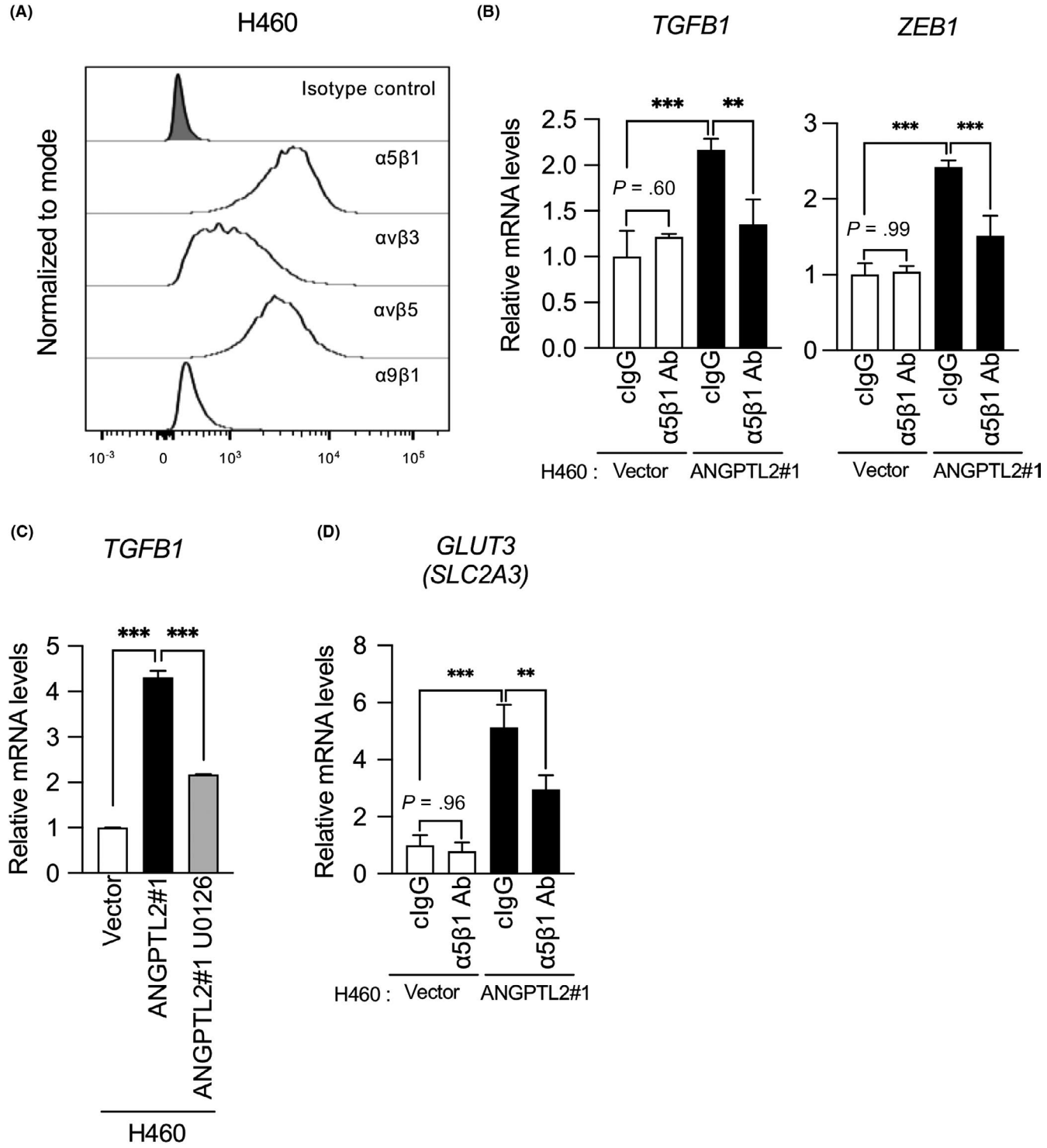

FIGURE 4 Angiopoietin-like protein 2 (ANGPTL2) induces zinc finger E-box binding homeobox 1 (ZEB1)-dependent glucose transporter 3 (GLUT3) expression through integrin α5β1. A, Typical profiles of cell surface expression of integrins in H460 cells, as assessed by flow cytometry. Gating of living cells was carried out after background assessment. B, Comparison of levels of indicated transcripts in H460/ANGPTL2 and H460/vector cells treated with integrin α5β1-blocking Ab or control IgG (cIgG). Levels in H460/vector cells treated with control IgG were set to 1. Data are means ± SD; n = 3 per group. $^{**}P < .01$, $^{***}P < .001$, one-way ANOVA followed by Tukey's multiple comparison test. C, Comparison of levels of *TGFB1* transcripts in H460/ANGPTL2 and H460/vector control cells, either nontreated or treated with the MEK inhibitor U0126. Levels in vector control cells were set to 1. Data are means ± SD; n = 3 per group. $^{***}P < .001$, one-way ANOVA followed by Tukey's multiple comparison test. D, Comparison of levels of GLUT3 (*SLC2A3*) transcripts in H460/ANGPTL2 and H460/vector cells treated with integrin α5β1-blocking Abs or cIgG. Levels in H460/vector cells treated with control IgG were set to 1. Data are means ± SD; n = 3 per group. $^{**}P < .01$, $^{***}P < .001$, one-way ANOVA followed by Tukey's multiple comparison test

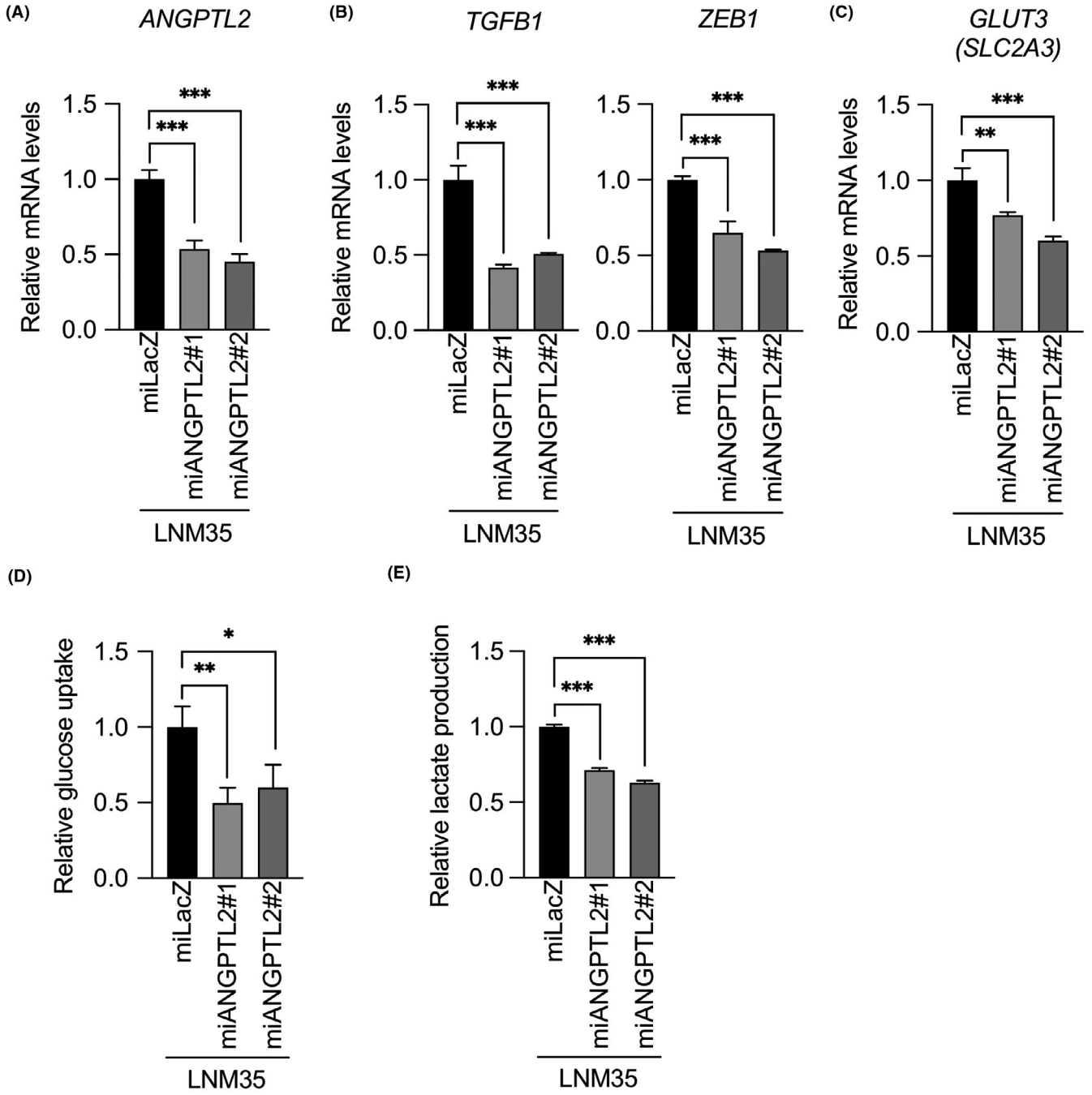

FIGURE 5 Angiopoietin-like protein 2 (ANGPTL2) knockdown in lung cancer cells decreases glycolytic metabolism. A-C, Comparison of levels of indicated transcripts in ANGPTL2 knockdown (miANGPTL2#1 and miANGPTL2#2) and control (miLacZ) LNM35 cells. Levels in control cells were set to 1. Data are means ± SD; n = 3 per group. $^{**}P < .01$, $^{***}P < .001$, one-way ANOVA followed by Tukey's multiple comparison test. D, Relative glucose uptake in ANGPTL2 knockdown and control LNM35 lines. Levels in control cells were set to 1. Data are means ± SD; n = 3 per group. $^{*}P < .05$, $^{**}P < .01$, one-way ANOVA followed by Tukey's multiple comparison test. E, Relative lactate production in ANGPTL2 knockdown and control LNM35 lines. Levels in control cells were set to 1. Data are means ± SD; n = 3 per group. $^{***}P < .001$, one-way ANOVA followed by Tukey's multiple comparison test

3.6 | Angiopoietin-like protein 2 expression in primary tumor tissues correlates with GLUT3 expression

Finally, we assessed a potential correlation in *ANGPTL2*, *GLUT3*, and *ZEB1* mRNA expression levels in primary tumor tissues from 96 lung cancer patients (Figure 6A). *ANGPTL2* expression was positively correlated with *GLUT3* and *ZEB1* expression in these specimens ($r = .3536$ and $r = .5676$), whereas we observed no correlation between *ANGPTL2* and *GLUT1* expression in these samples ($r = .0716$). Furthermore, we observed a positive correlation between *ZEB1* and *GLUT3* expression in these specimens ($r = .6788$).

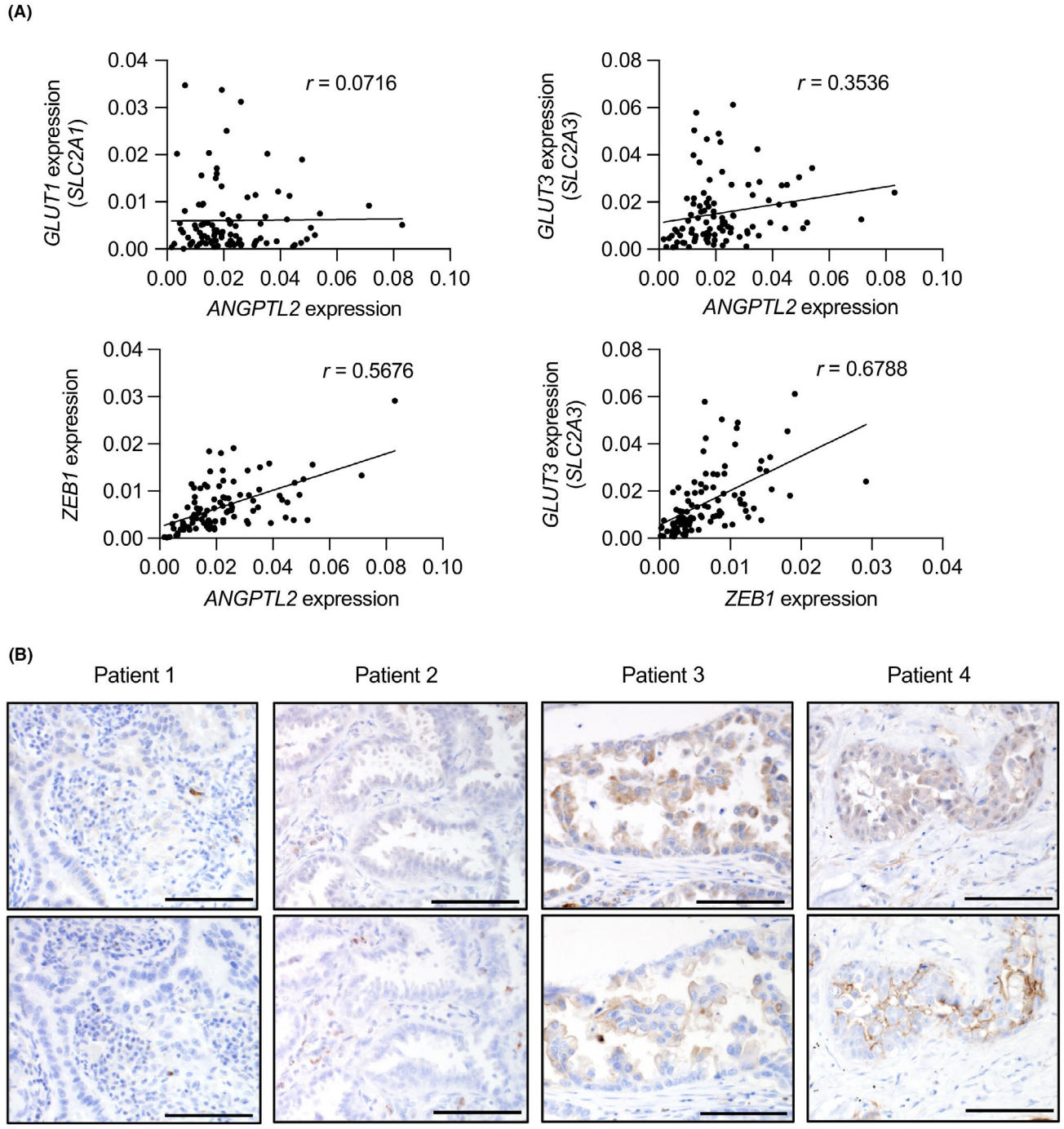

FIGURE 6 Angiopoietin-like protein 2 (ANGPTL2) expression correlates with glucose transporter 3 (GLUT3) expression in human lung cancer. A, Correlation between (upper) *ANGPTL2* and GLUT1 (*SLC2A1*) or *ANGPTL2* and GLUT3 (*SLC2A3*) or (lower) *ZEB1* and *ANGPTL2* or *ZEB1* and GLUT3 (*SLC2A3*) expression in primary tumor tissues from lung cancer patients (n = 96). Relative transcript abundance was normalized to that of *RPS18* mRNA. Spearman's correlation coefficient (*r*) was calculated as 0.0716 (upper left), 0.3536 (upper right), 0.5676 (lower left), and 0.6788 (lower right). B, Immunostaining for ANGPTL2 and GLUT3 in surgical specimens of primary tumors from 4 indicated patients with lung cancer. Scale bar = 100 μm

Immunohistochemical analysis of surgical specimens of primary tumors from patients with lung cancer using anti-ANGPTL2 and anti-GLUT3 Abs revealed relatively less GLUT3 expression in tumor tissues expressing low ANGPTL2 protein (Figure 6B, patients 1 and 2). By contrast, lung cancer cells expressing abundant ANGPTL2 protein showed high GLUT3 expression (Figure 6B, patients 3 and 4).

4 | DISCUSSION

Here, we provide evidence supporting a role for tumor cell-derived ANGPTL2 in promoting glycolytic metabolism in lung cancer cells. We report that a highly metastatic subline of a human large-cell lung carcinoma cell line showing high ANGPTL2 expression showed

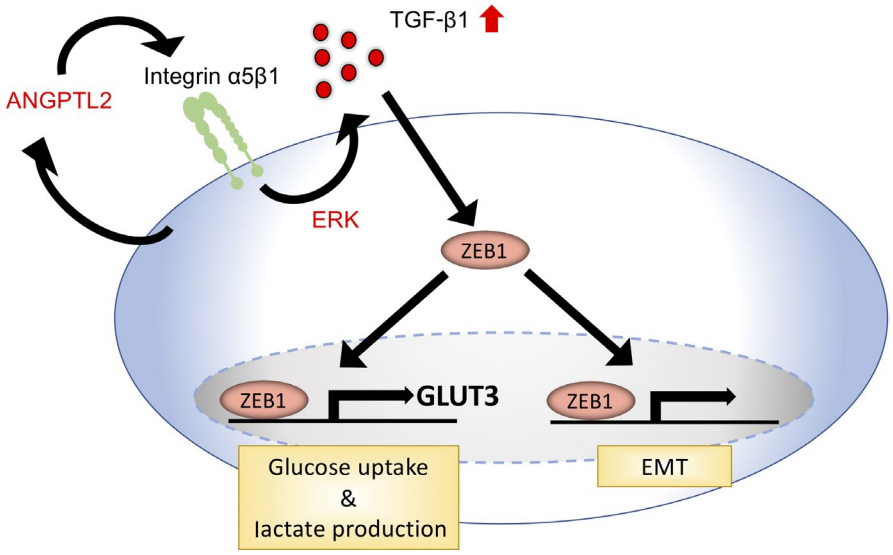

FIGURE 7 Model of proposed molecular mechanism underlying angiopoietin-like protein 2 (ANGPTL2)-mediated metabolic reprogramming. In lung cancer cells, tumor cell-derived ANGPTL2 activates the transforming growth factor-β (TGF-β)-zinc finger E-box binding homeobox 1 (ZEB1) pathway through integrin α5β1-ERK and induces not only the epithelial-mesenchymal transition (EMT) but also glucose transporter 3 (GLUT3) expression, enhancing glycolytic metabolism

enhanced glycolytic metabolism and increased GLUT3 expression compared with the less metastatic parental line. Mechanistically, through autocrine/paracrine signaling, tumor cell-derived ANGPTL2 signaling through integrin α5β1–ERK signaling increased expression of GLUT3 and glycolytic metabolism by activating the TGF-β-ZEB1 pathway in tumor cells. Conversely, ANGPTL2 suppression in tumor cells decreased GLUT3 expression and blocked glycolytic metabolism. Notably, we observed a positive correlation between ANGPTL2 and GLUT3 expression in primary tumors from patients with lung cancer. Overall, our findings show that tumor cell-derived ANGPTL2 signaling increases GLUT3 expression through the TGF-β-ZEB1 pathway, enhancing glycolytic metabolism (Figure 7).

The tumor microenvironment, which is characterized by hypoxia and/or undernutrition, accelerates production of tumor cell-derived humoral factors, such as cytokines and growth factors, leading to the EMT in tumor cells.[29,30] Epithelial-mesenchymal transition-dependent tumor invasion and metastasis is accompanied by increased cancer cell stemness and drug resistance.[31] Furthermore, more recent studies report that the EMT is associated with altered metabolism in cancer cells[32] and that EMT-induced metabolic reprogramming in favor of glycolytic phenotypes promotes tumor aggressiveness.[33] We previously showed that hypoxia and undernutrition increase ANGPTL2 expression in tumor cells and thereby enhance tumor cell metastatic capacity.[19] The present study now shows that ANGPTL2 induces not only the EMT but also metabolic reprogramming in lung cancer cells through activating the TGF-β pathway. These findings show that, in the tumor microenvironment, tumor cell-derived ANGPTL2 serves as an important mediator of both EMT induction and metabolic reprogramming in tumor cells, enhancing tumor aggressiveness.

Mechanistically, we reveal here that activation of ANGPTL2-dependent glycolytic metabolism is attributable to TGF-β signaling activated in tumor cells. Accordingly, we previously reported that ANGPTL2 upregulates TGF-β expression through integrin α5β1-ERK signaling in renal tubular epithelial cells and macrophages.[28] Moreover, we also reported that ANGPTL2 increases TGF-β expression through the integrin α5β1-p38-MAPK pathway in osteosarcoma cells.[21] Our findings strongly suggest that ANGPTL2 activity upregulates TGF-β expression through integrin α5β1-ERK signaling. Hence, we conclude that ANGPTL2-activated ERK and/or p38 MAPK signaling contributes to activation of the TGF-β pathway in lung cancer cells, thereby increasing ZEB1 and GLUT3 expression and activating glycolytic activity. Interestingly, others report that nuclear factor-κB (NF-κB) contributes to *ZEB1* induction in cancer cells[34] and that NF-κB increases *GLUT3* expression in cancer cells.[35] Because ANGPTL2-integrin α5β1 signaling activates the NF-κB pathway in tumor cells,[21] it is now of interest to investigate whether NF-κB functions in ANGPTL2-integrin α5β1 signaling-mediated upregulation of *GLUT3* expression in lung cancer cells.

To produce ATP as energy and to maintain cellular survival, non-tumor epithelial cells rely primarily on mitochondrial oxidative phosphorylation. In contrast, cancer cells produce ATP primarily through glycolysis, regardless of whether cellular conditions are aerobic or not, a metabolic switch known as the Warburg effect.[36,37] Enhanced glycolytic metabolism seen in cancer cells is due to induction of glycolysis-related genes, including GLUT factors.[38] Glucose transporter 1 is reportedly expressed in various cancers, including brain, colon, and lung cancers, and contributes to glucose uptake in those tumor cells.[39-41] Similar to GLUT1, GLUT3 is also expressed in some cancers, including lung cancer.[27,41] Both GLUT1 and GLUT3 expression in tumor cells reportedly correlates with poor prognosis of lung cancer patients.[9] Conversely, several studies report that suppressing GLUT expression in tumor cells blocks tumor progression.[42,43] The present study indicates that ANGPTL2 expression is correlated with GLUT3 expression in primary tumors from patients with lung cancer. Moreover, our in vitro experiments using lung cancer lines reported here revealed that ANGPTL2 signaling increases GLUT3 expression and enhances glycolytic metabolism, whereas ANGPTL2 suppression decreased GLUT3 expression and antagonized glycolytic metabolism. These findings are consistent with our previous reports that ANGPTL2 expression in tumor cells correlates with metastatic ability and invasiveness of cancer cells and poor prognosis of cancer patients.[19] They also suggest

that ANGPTL2-dependent GLUT3 expression in tumor cells might underlie poor prognosis of lung cancer patients both by activating glycolytic metabolism and increasing cancer malignancy.

In summary, we show that tumor cell-derived ANGPTL2 enhances glycolytic metabolism in lung cancer cells by increasing *GLUT3* expression through the integrin α5β1-TGF-β-ZEB1 pathway. We also show that ANGPTL2 knockdown inactivates glycolytic metabolism in lung cancer cells. Based on these findings, we propose that tumor cell-derived ANGPTL2 regulates the preference for glycolytic metabolism in cancer cells. Taken together with our previous reports that ANGPTL2 promotes aggressive metastatic phenotypes by activating tumor cell motility and invasiveness and the EMT, tumor cell-derived ANGPTL2 could be a therapeutic target useful to antagonize cancer malignancy.

ACKNOWLEDGMENTS

We thank Kiyoka Tabu, Noriko Shirai, and Ayaka Yoshida for technical assistance. We also thank Dr Adi F. Gazdar (University of Texas Southwestern Medical Center) for the gift of the HCC15 cell line. This work was supported by the Scientific Research Fund of the Ministry of Education, Culture, Sports, Science and Technology (MEXT) of Japan (grant no. 17K08663 to M. Endo, grant no. 18K15246 to H. Horiguchi, and grant no. 18K07236 to T. Kadomatsu), the Core Research for Evolutional Science and Technology (CREST) program of the Japan Science and Technology Agency (JST) (grant no. 13417915 to Y. Oike), the CREST program of the Japan Agency for Medical Research and Development (AMED) (grant no. JP19gm0610007 to Y. Oike), and the Takeda Science Foundation (to Y. Oike and to T. Kadomatsu).

DISCLOSURE

The authors have no conflict of interest.

ORCID

Haruki Horiguchi https://orcid.org/0000-0001-9344-8362
Tsuyoshi Kadomatsu https://orcid.org/0000-0003-3327-6954

REFERENCES

1. Hanahan D, Weinberg RA. Hallmarks of cancer: the next generation. *Cell*. 2011;144(5):646-674.
2. Lunt SY, Vander Heiden MG. Aerobic glycolysis: meeting the metabolic requirements of cell proliferation. *Annu Rev Cell Dev Biol*. 2011;27:441-464.
3. DeBerardinis RJ, Lum JJ, Hatzivassiliou G, Thompson CB. The biology of cancer: metabolic reprogramming fuels cell growth and proliferation. *Cell Metab*. 2008;7(1):11-20.
4. Icard P, Shulman S, Farhat D, Steyaert J-M, Alifano M, Lincet H. How the Warburg effect supports aggressiveness and drug resistance of cancer cells? *Drug Resist Updat*. 2018;38:1-11.
5. Thorens B, Mueckler M. Glucose transporters in the 21st Century. *Am J Physiol Endocrinol Metab*. 2010;298(2):E141-E145.
6. Adekola K, Rosen ST, Shanmugam M. Glucose transporters in cancer metabolism. *Curr Opin Oncol*. 2012;24(6):650-654.
7. Flavahan WA, Wu Q, Hitomi M, et al. Brain tumor initiating cells adapt to restricted nutrition through preferential glucose uptake. *Nat Neurosci*. 2013;16(10):1373-1382.
8. Kim E, Jung S, Park WS, et al. Upregulation of SLC2A3 gene and prognosis in colorectal carcinoma: analysis of TCGA data. *BMC Cancer*. 2019;19(1):1-10.
9. Younes M, Brown RW, Stephenson M, Gondo M, Cagle PT. Overexpression of Glut1 and Glut3 in stage I nonsmall cell lung carcinoma is associated with poor survival. *Cancer*. 1997;80(6):1046-1051.
10. Thiery JP, Acloque H, Huang RYJ, Nieto MA. Epithelial-mesenchymal transitions in development and disease. *Cell*. 2009;139(5):871-890.
11. Miettinen PJ, Ebner R, Lopez AR, Derynck R. TGF-beta induced transdifferentiation of mammary epithelial cells to mesenchymal cells: involvement of type I receptors. *J Cell Biol*. 1994;127(6 Pt 2):2021-2036.
12. Tan E-J, Olsson A-K, Moustakas A. Reprogramming during epithelial to mesenchymal transition under the control of TGFbeta. *Cell Adh Migr*. 2015;9(3):233-246.
13. Peinado H, Quintanilla M, Cano A. Transforming growth factor beta-1 induces snail transcription factor in epithelial cell lines: mechanisms for epithelial mesenchymal transitions. *J Biol Chem*. 2003;278(23):21113-21123.
14. Liu Y, El-Naggar S, Darling DS, Higashi Y, Dean DC. Zeb1 links epithelial-mesenchymal transition and cellular senescence. *Development*. 2008;135(3):579-588.
15. Pastushenko I, Blanpain C. EMT transition states during tumor progression and metastasis. *Trends Cell Biol*. 2019;29(3):212-226.
16. Sciacovelli M, Frezza C. Metabolic reprogramming and epithelial-to-mesenchymal transition in cancer. *FEBS J*. 2017;284(19):3132-3144.
17. Aoi J, Endo M, Kadomatsu T, et al. Angiopoietin-like protein 2 accelerates carcinogenesis by activating chronic inflammation and oxidative stress. *Mol Cancer Res*. 2014;12(2):239-249.
18. Aoi J, Endo M, Kadomatsu T, et al. Angiopoietin-like protein 2 is an important facilitator of inflammatory carcinogenesis and metastasis. *Cancer Res*. 2011;71(24):7502-7512.
19. Endo M, Nakano M, Kadomatsu T, et al. Tumor cell-derived angiopoietin-like protein ANGPTL2 is a critical driver of metastasis. *Cancer Res*. 2012;72(7):1784-1794.
20. Masuda T, Endo M, Yamamoto Y, et al. ANGPTL2 increases bone metastasis of breast cancer cells through enhancing CXCR4 signaling. *Sci Rep*. 2015;5:9170.
21. Odagiri H, Kadomatsu T, Endo M, et al. The secreted protein ANGPTL2 promotes metastasis of osteosarcoma cells through integrin alpha5beta1, p38 MAPK, and matrix metalloproteinases. *Sci Signal*. 2014;7(309):ra7.
22. Kozaki K, Miyaishi O, Tsukamoto T, et al. Establishment and characterization of a human lung cancer cell line NCI-H460-LNM35 with consistent lymphogenous metastasis via both subcutaneous and orthotopic propagation. *Cancer Res*. 2000;60(9):2535-2540.
23. Girard L, Zochbauer-Muller S, Virmani AK, Gazdar AF, Minna JD. Genome-wide allelotyping of lung cancer identifies new regions of allelic loss, differences between small cell lung cancer and non-small cell lung cancer, and loci clustering. *Cancer Res*. 2000;60(17):4894-4906.
24. Kubota Y, Oike Y, Satoh S, et al. Cooperative interaction of Angiopoietin-like proteins 1 and 2 in zebrafish vascular development. *Proc Natl Acad Sci USA*. 2005;102(38):13502-13507.
25. Bonatelli M, Silva ECA, Carcano FM, et al. The Warburg effect is associated with tumor aggressiveness in testicular germ cell tumors. *Front Endocrinol (Lausanne)*. 2019;10:417.
26. Masin M, Vazquez J, Rossi S, et al. GLUT3 is induced during epithelial-mesenchymal transition and promotes tumor cell proliferation in non-small cell lung cancer. *Cancer Metab*. 2014;2:11.
27. Ancey PB, Contat C, Meylan E. Glucose transporters in cancer – from tumor cells to the tumor microenvironment. *FEBS J*. 2018;285(16):2926-2943.

28. Morinaga J, Kadomatsu T, Miyata K, et al. Angiopoietin-like protein 2 increases renal fibrosis by accelerating transforming growth factor-beta signaling in chronic kidney disease. *Kidney Int*. 2016;89(2):327-341.
29. Jiang J, Tang Y, Liang X. EMT: a new vision of hypoxia promoting cancer progression. *Cancer Biol Ther*. 2011;11(8):714-723.
30. Landskron G, De la Fuente M, Thuwajit P, Thuwajit C, Hermoso MA. Chronic inflammation and cytokines in the tumor microenvironment. *J Immunol Res*. 2014;2014:149185.
31. Xiao D, He J. Epithelial mesenchymal transition and lung cancer. *J Thorac Dis*. 2010;2(3):154-159.
32. Liu M, Quek L-E, Sultani G, Turner N. Epithelial-mesenchymal transition induction is associated with augmented glucose uptake and lactate production in pancreatic ductal adenocarcinoma. *Cancer Metab*. 2016;4:19.
33. Kang H, Kim H, Lee S, Youn H, Youn B. Role of metabolic reprogramming in epithelial-mesenchymal transition (EMT). *Int J Mol Sci*. 2019;20(8): E2042. https://doi.org/10.3390/ijms20082042.
34. Rajabi H, Alam M, Takahashi H, et al. MUC1-C oncoprotein activates the ZEB1/miR-200c regulatory loop and epithelial-mesenchymal transition. *Oncogene*. 2014;33(13):1680-1689.
35. Zha X, Hu Z, Ji S, et al. NFkappaB up-regulation of glucose transporter 3 is essential for hyperactive mammalian target of rapamycin-induced aerobic glycolysis and tumor growth. *Cancer Lett*. 2015;359(1):97-106.
36. Warburg O. On the origin of cancer cells. *Science*. 1956;123(3191):309-314.
37. Vander Heiden MG, Cantley LC, Thompson CB. Understanding the Warburg effect: the metabolic requirements of cell proliferation. *Science*. 2009;324:1029-1033.
38. Macheda ML, Rogers S, Best JD. Molecular and cellular regulation of glucose transporter (GLUT) proteins in cancer. *J Cell Physiol*. 2005;662:654-662.
39. Glucose transport: meeting the metabolic demands of cancer, and applications in glioblastoma treatment. *Am J Cancer Res*. 2016;6(8):1599-1608.
40. Haber RS, Rathan A, Weiser KR, et al. GLUT1 glucose transporter expression in colorectal carcinoma: a marker for poor prognosis. *Cancer*. 1998;83(1):34-40.
41. Kurata T, Oguri T, Isobe T, Ishioka S, Yamakido M. Differential expression of facilitative glucose transporter (GLUT) genes in primary lung cancers and their liver metastases. *Jpn J Cancer Res*. 1999;90(11):1238-1243.
42. Liu Y, Cao Y, Zhang W, et al. A small-molecule inhibitor of glucose transporter 1 downregulates glycolysis, induces cell-cycle arrest, and inhibits cancer cell growth in vitro and in vivo. *Mol Cancer Ther*. 2012;11(8):1672-1682.
43. Chan DA, Sutphin PD, Nguyen P, et al. Targeting GLUT1 and the Warburg effect in renal cell carcinoma by chemical synthetic lethality. *Sci Transl Med*. 2011;3(94):94ra70.

SUPPORTING INFORMATION

Additional supporting information may be found online in the Supporting Information section.

How to cite this article: Osumi H, Horiguchi H, Kadomatsu T, et al. Tumor cell-derived angiopoietin-like protein 2 establishes a preference for glycolytic metabolism in lung cancer cells. *Cancer Sci*. 2020;111:1241–1253. https://doi.org/10.1111/cas.14337